An Imageable Metastatic Treatment Model of Nasopharyngeal Carcinoma

Tengfei Liu,[1,2] Yanqin Ding,[1] Weibing Xie,[1] Zuguo Li,[1] Xiaoyan Bai,[1] Xin Li,[1] Weiyi Fang,[1] Caiping Ren,[2] Shuang Wang,[1] Robert M. Hoffman,[3,4] and Kaitai Yao[1,2]

Abstract

Purpose: Nasopharyngeal carcinoma is highly prevalent in southern China and is often resistant to current treatment options.

Experimental Design: Clinically relevant mouse models are necessary for further understanding and drug discovery in this disease. Two nasopharyngeal carcinoma cell lines, stably expressing green fluorescent protein (GFP), 5-8F-GFP and 6-10B-GFP, were established. The cells were orthotopically injected into the nasopharynx or ectopically into the subcutis of nude mice. Whole-body fluorescence imaging was used to monitor the growth of the primary tumor as well as angiogenesis and metastasis.

Results: The metastatic behavior of 5-8F and 6-10B were distinct in the orthotopic model. Orthotopic implantation of highly metastatic 5-8F cells resulted in brain invasion, cervical lymph node metastases, and pulmonary metastases similar to what is often observed in patients. Cell line 6-10B was less metastatic, which occasionally resulted in pulmonary metastasis. GFP enabled imaging of micrometastasis. Neither 5-8F nor 6-10B were metastatic in the s.c. site. These results indicated that, in addition to the cancer cell type, the host microenvironment was critical for metastasis to occur consistent with the "seed-and-soil" hypothesis. 5-8F was highly sensitive to 5-fluorouracil (5-FU), whereas 6-10B was moderately sensitive.

Conclusions: The imageable orthotopic model should play a critical role in elucidating the mechanisms involved in the growth, progression, metastasis, and angiogenesis of nasopharyngeal carcinoma and for evaluation of novel compounds with potential efficacy.

Nasopharyngeal carcinoma (NPC) is endemic in a few well-defined populations, mostly in South China, Hong Kong, Taiwan, and Singapore. NPC was the fourth most common new malignancy in Hong Kong. NPC arises in the epithelial lining of the nasopharynx. NPC is classified into three histologic types: keratinizing squamous cell carcinoma (type I); and nonkeratinizing carcinoma, characterized as differentiated (type II) or undifferentiated (type III). Type III NPC comprises more than 95% of NPC in high-incidence areas, and most of the remaining 5% is type II NPC. In contrast, type I NPC is predominant in low-incidence regions and may have an etiology distinct from that of the other two histologic types (1). The etiology of NPC is poorly understood. Epstein-Barr virus (EBV) is associated with NPC, but its role is also not clear. The biology of NPC is also poorly understood, and treatment outcome is dismal. Better models could solve these two related problems of NPC.

Previous models of NPC involved ectopic s.c. implantation of NPC human tumor tissue in immunodeficient mice (2–5). Such models differed significantly from the original donor tumors. For example, such tumors became encapsulated and did not metastasize. Also, the important early stages of tumor development were essentially hidden. Orthotopic models of many tumor types have been developed which metastasize in a similar manner as in patients (6). Fluorescent proteins such as the green fluorescent protein (GFP) and red fluorescent protein have been used to image primary tumor growth and metastases in the orthotopic models (7). A major advantage of GFP-expressing tumor cells is that imaging requires no preparative procedures, contrast agents, substrates, or anesthesia, as do other imaging techniques (8). GFP imaging is thus uniquely appropriate for whole-body imaging of tumor growth and metastases in live animals (9–11). The GFP images have revealed microscopic stages of tumor growth and metastatic seeding, often down to the single-cell level. Most importantly, the ability to follow tumor cells in a relatively noninvasive manner in the intact animal makes previously unobtainable precision in the studies of tumor behavior and response to chemotherapeutic agents possible (12–15).

Authors' Affiliations: [1]Cancer Institute, Nanfang Hospital, Southern Medical University, Key Laboratory of Transcriptomics and Proteomics of Human Diseases; [2]Cancer Research Institute, Xiang-Ya School of Medicine, Central South University, Guangzhou, China; [3]AntiCancer, Inc.; and [4]Department of Surgery, University of California – San Diego, San Diego, California

Received 1/15/07; revised 3/9/07; accepted 3/21/07.

Grant support: National High Technology Research and Development Program of China (Program 863; 2001AA216101 and 2003AA216010) and National Key Science and Technology Research Program of Guandong Province (2003A308401). The Cancer Institute, Nanfang Hospital, Nanfang Medical University, Key Laboratory of Transcriptomics and Proteomics of Human Diseases is supported by the Ministry of Education and Guangdong Province, Guangdong Provincial Key Laboratory of Molecular Tumor Pathology, Guangzhou, China.

The costs of publication of this article were defrayed in part by the payment of page charges. This article must therefore be hereby marked *advertisement* in accordance with 18 U.S.C. Section 1734 solely to indicate this fact.

Requests for reprints: Robert M. Hoffman, AntiCancer, Inc., San Diego, CA 92111. Phone: 1-858-654-2555; Fax: 1-858-268-4175; E-mail: all@anticancer.com.

doi:10.1158/1078-0432.CCR-07-0089

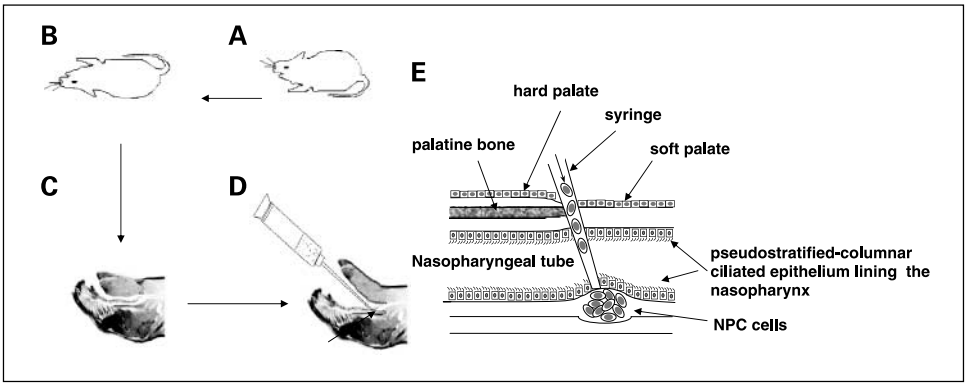

Fig. 1. Illustration demonstrating the implantation method. *A,* mouse under normal conditions. *B,* anesthetized mouse. *C,* preinoculation. *D,* nasopharyngeal orthotopic inoculation. *E,* tissue details of nasopharyngeal orthotopic inoculation.

Angiogenesis is a fundamental requirement for tumor growth, progression, and metastasis. Therefore, angiogenesis has become a critical target for cancer chemotherapy (16–18). Blood vessels in GFP-expressing tumors can be detected by their strong nonluminous contrast and appear as sharply defined dark networks against the bright GFP fluorescence.

In this report, using stable and high GFP-expressing NPC cell lines, we established and describe imageable "patientlike" orthotopic human NPC models in nude mice. These new models revealed strong differences in metastatic potential and drug response between NPC cell lines. The models should be of important use to understand the biology of metastatic NPC and for the discovery of effective therapy for this disease.

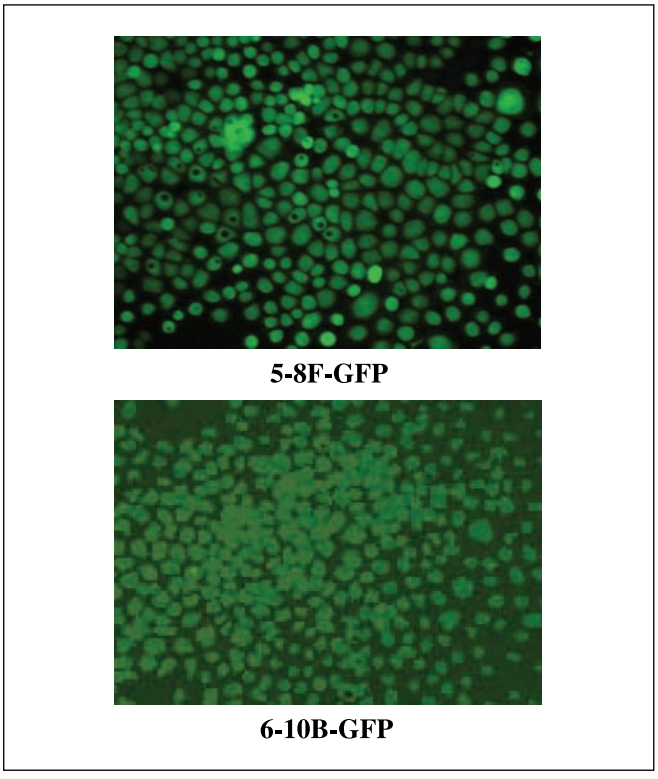

Fig. 2. Stable, high-level GFP-expressing human NPC cell line transfectants *in vitro*. Cell lines were transfected with pGFP-N1, which expresses the GFP and neomycin resistance genes. Stable, high-expression clones were selected in up to 2,000 μg/mL G418.

Materials and Methods

Cell lines. Highly tumorigenic and metastatic NPC cell line 5-8F and tumorigenic but low-metastatic NPC cell line 6-10B were obtained from the Cancer Center of Sun Yat-sen University. Cells were maintained in RPMI 1640 supplemented with 15% heat-inactivated fetal bovine serum. Cells were cultured at 37°C in a 5% CO_2 incubator. The 5-8F and 6-10B cell lines are sensitive to 5-fluorouracil (5-FU) and cisplatin [*cis*-diaminedichloroplatinum (CDDP)] *in vitro*.

Animals. Nude *nu/nu* mice were maintained in a barrier facility in racks filtered with high-efficiency particulate air filter. The animals were fed with an autoclaved laboratory rodent diet. The mice in this study were supplied by the Experimental Animal Centre of NanFang Medical University, which is certified by the Guandong Provincial Bureau of Science. All animal experiments involved ethical and humane treatment under a license from the Guandong Provincial Bureau of Science.

GFP transfection. 5-8F and 6-10B cells were cultured in growth medium (without antibiotics) to 90% to 95% confluence at the time of transfection (2×10^5 cells per well in 24-well plates). GFP-N1 DNA was diluted in 50 μL of Opti-MEM medium without serum and mixed gently. LipofectAMINE 2000 was diluted in 50 μL of Opti-MEM, mixed gently, and incubated for 5 min at room temperature. After 5 min of incubation, the dilute DNA was combined with dilute LipofectAMINE 2000 (total volume is 100 μL), mixed gently, and incubated for 20 min at room temperature to permit the formation of the DNA-Lipofect-AMINE 2000 complexes. About 100 μL DNA-LipofectAMINE 2000 complexes were added to each well and mixed gently by rocking the plate back and forth. Cells were incubated in an incubator with 5% CO_2 at 37°C. After 6 h, complexes were removed and replaced with the growth medium. After 24 to 48 h, the transient transfection efficiency was determined using an Olympus fluorescence microscope. Then, cells were passaged at appropriate ratios in six-well plates. The next day, cells were cultured in the presence of 500 to 2,000 μg/mL of G418 (Life Technology) increased in a stepwise manner for 10 days for selection of highly expressing GFP cells.

Doubling time of stable enhanced green fluorescent protein clones and parental cells. 5-8F and 6-10B parental cells and GFP-expressing clones were seeded at 1×10^4 in 24-well plates. Cells were harvested and counted every 24 h using a hemocytometer (Reichert Scientific Instruments, Buffalo, NY). The doubling time was calculated from the cell growth curve over 7 days.

Cell cycle phase distribution of pre- and post-transfection of GFP. 5-8F and 6-10B parental cells and GFP-expressing clones were cultured in RPMI 1640 (Life Technology, Inc.) containing 15% FCS (PAA). Cells were harvested with trypsinization, washed thrice with cold 1% 0.01 mol/L PBS, suspended with cold 70% ethanol, and stored at -20°C. Flow cytometry analysis was then done.

S.c. tumor growth. Six-week-old BALB/c *nu/nu* mice were injected s.c. with a single dose of 1×10^6 5-8F or 6-10B parental cells and their corresponding GFP transfectants, respectively. Serum-free medium was

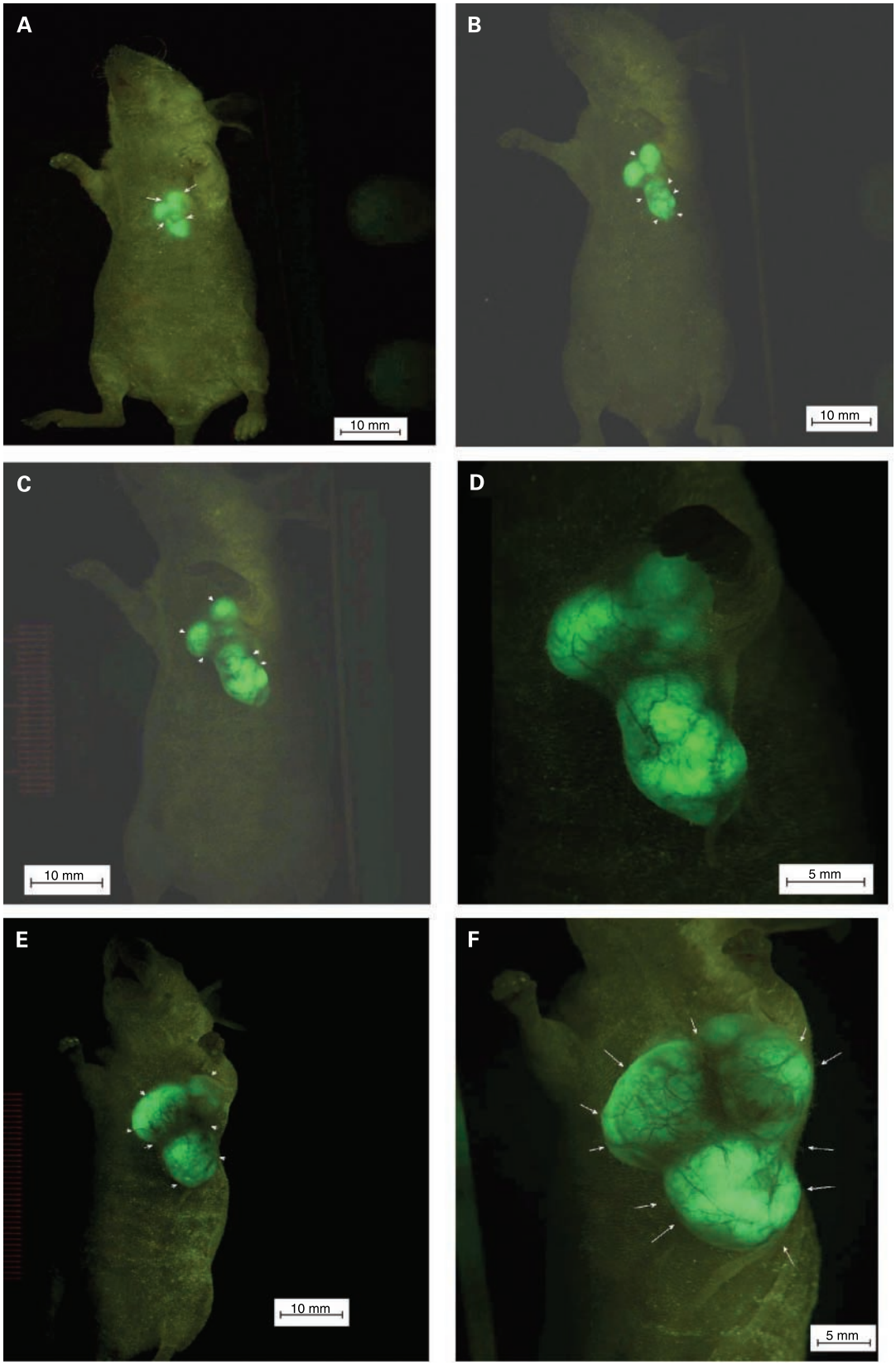

Fig. 3. Time course of external imaging of angiogenesis of s.c. NPC. Human NPC cell line 5-8F-GFP was injected s.c. and imaged as described in Materials and Methods. *A,* day 7; bar, 10 mm. *B,* day 10; bar, 10 mm. *C,* day 14; bar, = 10 mm. *D,* day 20; bar, 5 mm. *E,* day 25; bar, 10 mm. *F,* day 35; bar, 5 mm.

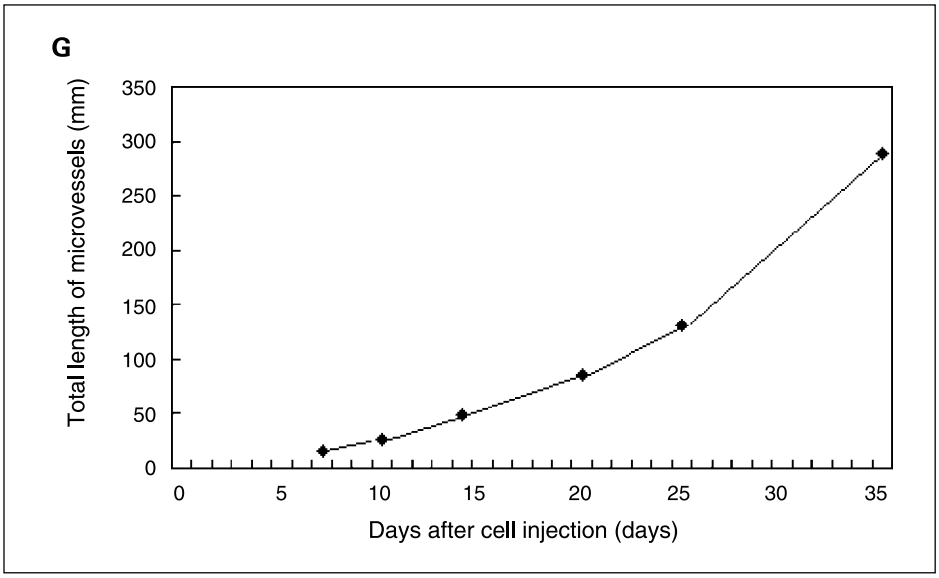

Fig. 3 *Continued. G,* quantitative graph of microvessel density as a function of time.

Fig. 4. Imaging 5-8F-GFP NPC metastases. *A,* bright-field photo; black arrow, swelling cervical lymph node. *B,* whole-body image of cervical lymph node metastasis (*white arrows*). *C,* open image of lung micrometastases (*white arrows*). Cervical lymph node metastasis is also visualized (*arrowhead*). *D,* metastatic lesions are seen in the brain by open GFP imaging.

Table 1. Metastatic pattern of orthotopic models of human NPC in nude mice

Cell line	Numbers of animals							
	Total animals	Animals with tumors	Brain metastasis	Cervical lymph node metastasis	Lung metastasis	Brain and lung metastasis	Cervical lymph node and lung metastasis	Brain, cervical lymph node, and lung metastasis
6-10B	20	20	0	0	0	0	0	0
5-8F	20	18	5	15	17	5	14	3

used for cell implantation. Cells were first harvested by trypsinization and washed thrice with cold serum-containing medium and then kept on ice. Cells were injected in a total volume of 0.5 mL within 40 min of harvesting.

Orthotopic injection and analysis of metastases. 5-8F and 6-10B GFP clones were cultured in RPMI 1640 (Life Technology, Inc.) containing 15% FCS (PAA) in 150-mL bottles. The cells were harvested by trypsinization and counted using a hemocytometer (Reichert Scientific Instruments). About 1×10^6 cells were injected in the nasopharynx orthotopically in nude mice. Cells were injected in a total volume of 0.05 mL serum-free medium within 40 min of harvesting.

Orthotopic injection was through the hard palate. A 4-1/2 needle was used. The procedure was carried out under anesthesia. The anesthesia protocol was as follows: A 1% solution of pentobarbital sodium was prepared by using filtration through a 0.2-μm syringe filter (Life Sciences). Five minutes before the procedure, the experimental animal was anesthetized using a 1% solution of pentobarbital sodium corresponding to 100 mg/kg through an abdominal cavity injection. When the mouse was under deep anesthesia, its mouth was opened, and its tongue was pressed slightly. At that time, the cells were rapidly injected through the hard palate. All procedures were done under sterile conditions (Fig. 1).

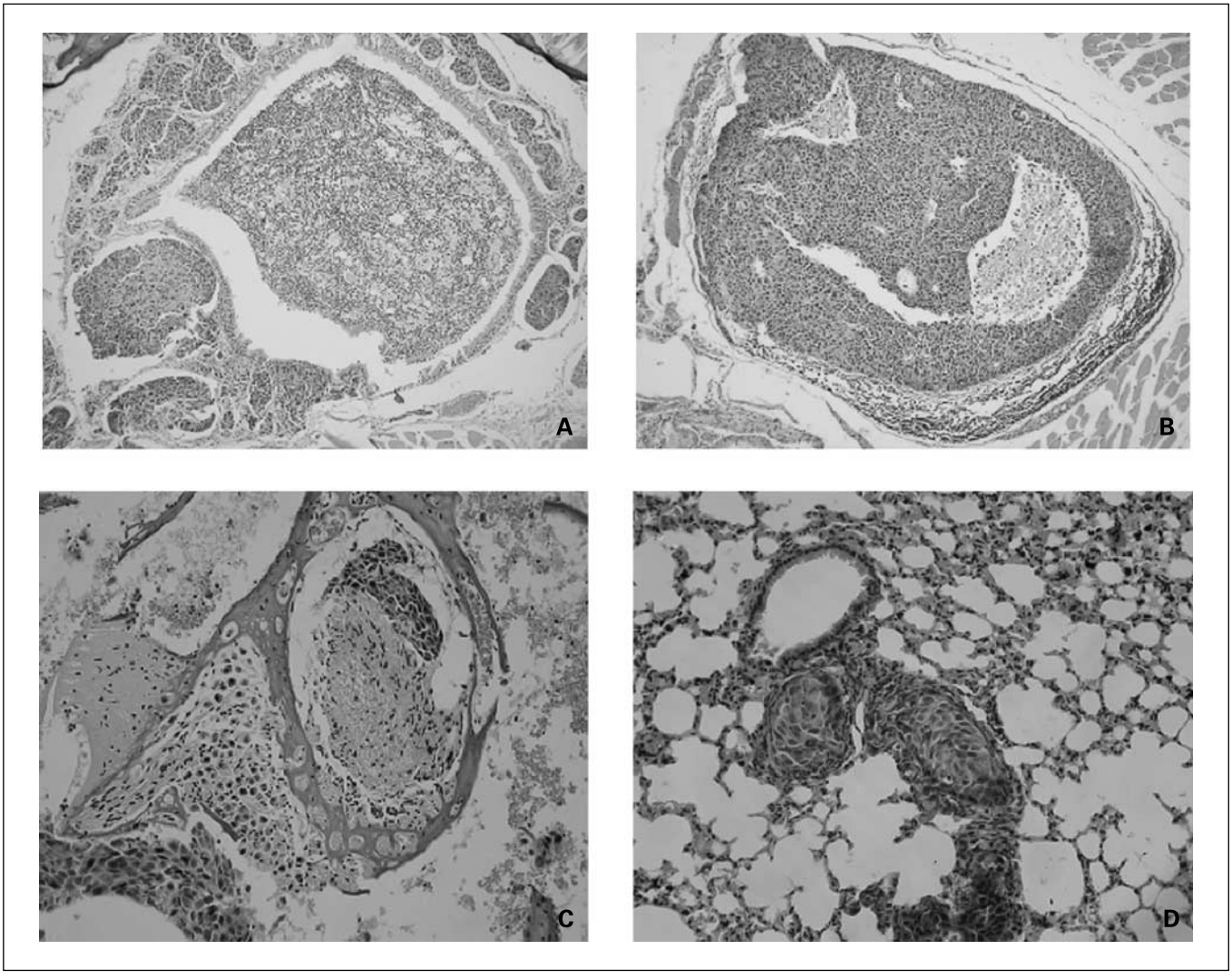

Fig. 5. Tissue sections stained with H&E show orthotopic NPC and its metastatic lesions. *A,* orthotopic primary NPC (H&E staining, ×400). *B,* lymph node metastasis (H&E staining, ×400). *C,* NPC invading the skull (H&E staining, ×400). *D,* lung metastasis (H&E staining, ×400).

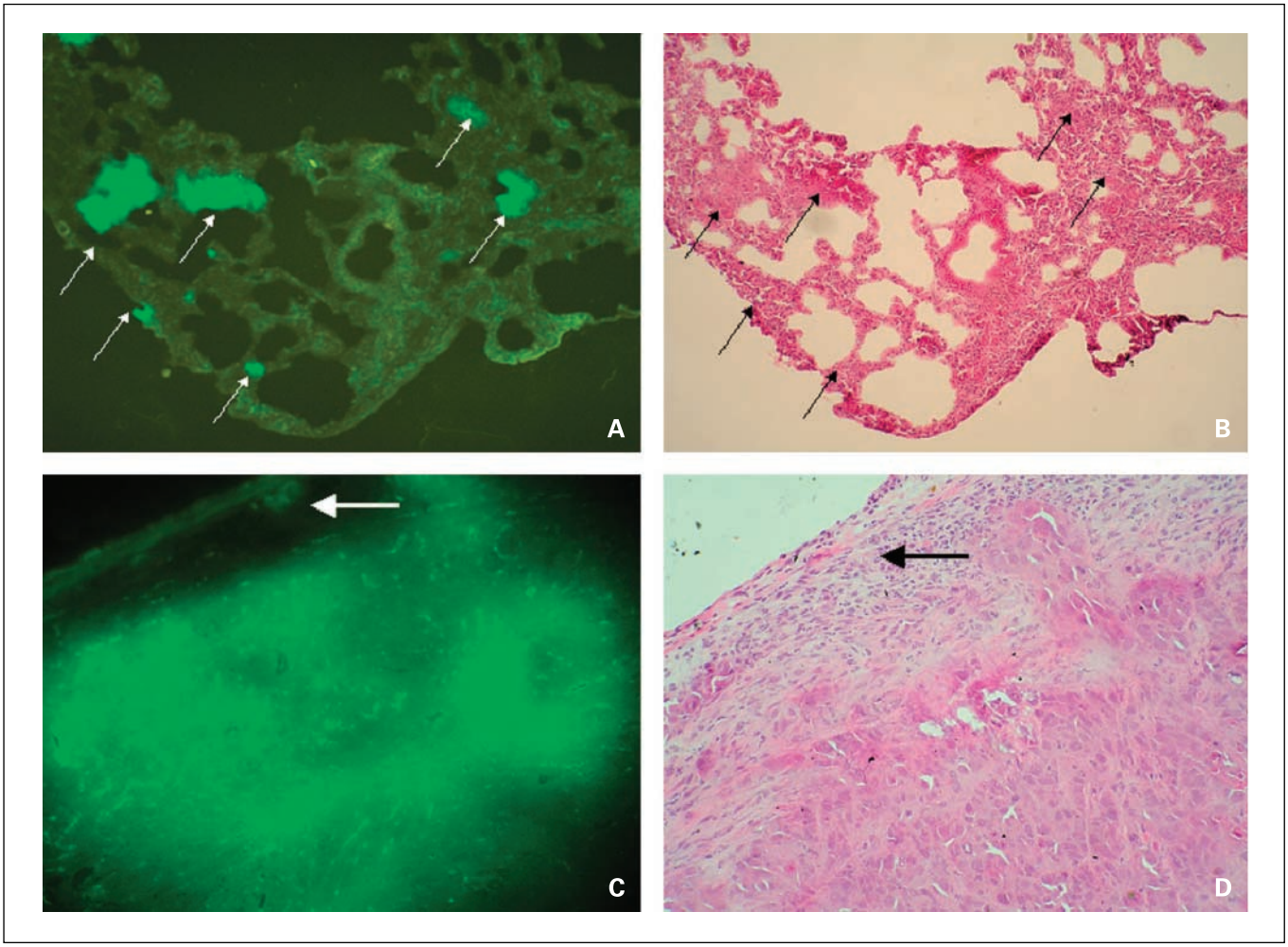

Fig. 6. Frozen sections of lung and lymph node metastases were observed under fluorescence microscopy. *A,* lung micrometastasis under fluorescence microscopy (*white arrows,* single cells; ×400). *B,* the same section as A (H&E staining, ×400). *C,* lymph node metastasis under fluorescence microscopy (*white arrow,* site of normal lymphocyte; ×400). *D,* the same section as *C* [*black arrow,* site seen in (*C*); H&E staining, ×400].

No post-implantation drugs were used to mitigate pain because the animals exhibited no signs of distress. No complications were observed with this methodology.

GFP whole-body imaging. A GFP whole-body image system (Lightools Research) equipped with two mercury 150-W lamp power supplies was used. Selective excitation of GFP was produced through a D470/40-nm band-pass filter. Emitted fluorescence was collected through a long-pass filter (D515 nm, Chroma Technology) on a cooled color charge-coupled-device camera (Retiga Exi Cooled CCD Camera, Q Imaging Co.). Images were processed for contrast and brightness and analyzed by IMAGE PRO PLUS 5.1 software (Media Cybernetics). High-resolution images of 1,392 × 1,040 pixels were captured, directly displayed on a monitor and digitally stored.

Drug treatment. The 6-10B model was treated with 5-FU at the following concentrations: 20, 30, and 40 mg/kg. CDDP was tested at 3 mg/kg with and without 20 mg/kg 5-FU. The 5-8F model was treated with 5-FU at the following concentrations: 30, 40, and 50 mg/kg. CDDP was tested in this model at 3 mg/kg with and without 40 mg/kg 5-FU. Normal saline was used as the negative control for both models.

When the average tumor diameter reached 4.0 mm, drug treatment was started. 5-FU was given daily for 5 days. CDDP was given daily for 3 days. The end point used in our studies was tumor weight. There were five mice per group. We used the SPSS 10.0 one-way Dunnett test to compare the treatment groups. A $P < 0.05$ for the treated groups compared with the untreated control indicated significance. Because statistical significance was achieved, the experiments were not repeated.

Results

Isolation of stable, high-level expression GFP transductants of 5-8F-GFP and 6-10B-GFP cells. GFP-transduced 5-8F and 6-10B cells were selected in multiple steps for growth in levels of Geneticin (G418) up to 2,000 mg/mL and for high GFP expression. The selected 5-8F-GFP and 6-10B-GFP cells had a strikingly bright GFP fluorescence that remained stable in the absence of selective agents after numerous passages (Fig. 2). There was no difference in the doubling times of parental cells and selected GFP transductants as determined by comparison with proliferation in monolayer cultures. There were also no differences in tumorgenic potential or cell cycle phase between parental cells and selected GFP transductants (data not shown).

Whole-body imaging of tumor growth and angiogenesis of s.c. NPC. 5-8F-GFP and 6-10B-GFP were injected s.c. A GFP whole-body imaging system visualized tumor growth and angiogenesis (Fig. 3). Although no metastasis was observed

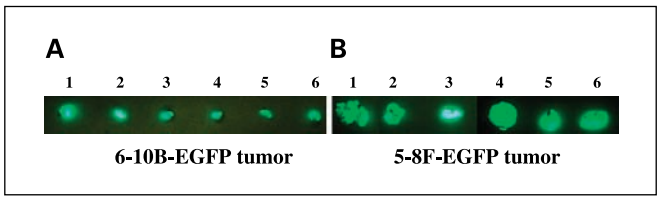

Fig. 7. GFP imaging of drug efficacy of NPC tumor models. Green fluorescence imaging shows tumor size after one cycle of chemotherapy as described in Materials and Methods, which also described the imaging procedures. *A,* 6-10B-EGFP tumor. 1, normal saline control; 2, 20 mg/kg 5-FU; 3, 30 mg/kg 5-FU; 4, 40 mg/kg 5-FU; 5, 20 mg/kg 5-FU + 3 mg/kg CDDP; 6, 3 mg/kg CDDP. *B,* 5-8F-EGFP tumor. 1, normal saline control; 2, 3 mg/kg CDDP; 3, 30 mg/kg 5-FU; 4, 40 mg/kg 5-FU; 5, 50 mg/kg 5-FU; 6, 40 mg/kg 5-FU + 3 mg/kg CDDP.

for either cell line after s.c. transplantation, the s.c. model was used to image angiogenesis because it was more feasible to image angiogenesis of s.c. tumors. We calculated the total vessel length in the region of the tumor that had the highest microviral density. Total vessel length increased over time (Fig. 3).

Whole-body imaging of orthotopic tumor growth and metastasis. 5-8F-GFP and 6-10B-GFP were injected orthotopically in nude mice. Whole-body imaging visualized the NPC tumors at the orthotopic site (Fig. 4). Brain, cervical lymph nodes, and lung metastases were imaged by GFP expression at high incidence with the high metastatic NPC cell line 5-8F-GFP. In contrast, only 2 of 20 mice had lung metastases with the low-metastatic NPC cell line 6-10B-GFP (Table 1, Fig. 4).

Histology. Poorly differentiated squamous cell carcinoma was found in orthotopic NPC, its metastatic lesions of the brain, cervical lymph nodes, and lung by H&E staining (Fig. 5). Frozen sections expressing GFP and H&E-stained slides were compared. GFP-expressing tumor cells could be distinguished by their bright fluorescence, often down to the single-cell level (Fig. 6).

Drug response. The two NPC models were treated with 5-FU and CDDP (Figs. 7 and 8). The 5-8F tumor was strongly inhibited by 5-FU: 30 mg/kg (IR [inhibition rate] = 61%), 40 mg/kg (IR = 69%), 50 mg/kg (82%). The combination of 5-FU (40 mg/kg) + 3 mg/kg CDDP had an IR of 86%. One-way Dunnett analysis for comparing tumor weights of experimental control groups resulted in $P = 0.001$ when comparing 5-FU at 30 mg/kg dose and untreated controls. The other doses of 5-FU had a $P < 0.001$ when compared with untreated controls (Table 2). Body weight differences between the groups were not significant, $P > 0.05$. CDDP at 3 mg/kg did not significantly inhibit tumor growth, nor was it toxic.

The response of the 6-10B model was moderately inhibited by 5-FU (Fig. 8; Table 2). The 30 mg/kg (IR = 36%), 40 mg/kg (IR = 55%), and the combination of 5-FU at 20 mg/kg + 3 mg/kg of CDDP had an IR of 68.38%. One-way Dunnett analysis resulted in $P = 0.011$, comparing 30 mg/kg 5-FU and control. A $P < 0.001$ was obtained for the other concentrations of 5-FU compared with control. Three mg/kg CDDP alone did not significantly inhibit tumor growth, with a P value of 0.142. The combination of 20 mg/kg 5-FU + 3 mg/kg CDDP inhibited tumor growth more effectively than 20 mg/kg 5-FU or 30 mg/kg 5-FU ($P < 0.05$). The difference between 20 mg/kg 5-FU + 3 mg/kg CDDP and 40 mg/kg 5-FU was not significant ($P = 0.30$).

The results showed that a 40 mg/kg 5-FU dose was more toxic than that of 20 mg/kg 5-FU + 3 mg/kg CDDP ($P = 0.000$). Toxicity included submucosal soft tissue edema in the mouth and mucoid degeneration and liver degeneration. The other visceral organs, including lung, kidneys, and stomach, were normal.

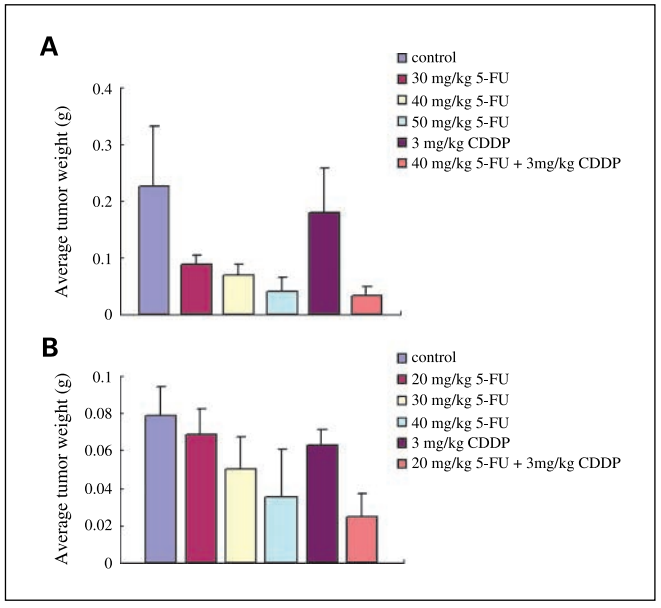

Fig. 8. *A,* efficacy of chemotherapy on the 5-8F NP model. *B,* efficacy of chemotherapy on the 6-10B NP model. See Materials and Methods for details.

Discussion

Using GFP expression in orthotopic models, we established a fluorescent orthotopic NPC metastatic model. This model closely simulates the clinical features of NPC growth, progression, and metastasis. Highly tumorigenic metastatic 5-8F cells manifested a pattern of brain invasion, cervical lymph node, and pulmonary metastases as observed in patients. In contrast, low-metastatic 6-10B cells did not manifest brain invasion or cervical lymph node metastases (Table 1). In s.c. models, neither cell line was metastatic. These results showed that the host microenvironment was critical for metastasis as described

Table 2. Efficacy of chemotherapy of NPC tumor models in nude mice

	Groups	
	6-10B	5-8F
	Tumor weights (grams)	
Normal saline control	0.2265 ± 0.1053	0.0787 ± 0.0158
20 mg/kg 5-FU		0.0688 ± 0.0136
30 mg/kg 5-FU	0.0877 ± 0.0176	0.0502 ± 0.0173
40 mg/kg 5-FU	0.0709 ± 0.0186	0.0357 ± 0.0254
50 mg/kg 5-FU	0.0404 ± 0.0236	
3 mg/kg CDDP	0.1792 ± 0.0790	0.0630 ± 0.0087
20 mg/kg 5-FU + 3 mg/kg CDDP		0.0249 ± 0.0120
40 mg/kg 5-FU + 3 mg/kg CDDP	0.0322 ± 0.0156	

in the "seed-and-soil" tumor metastatic hypothesis (19). Liver metastasis was not found in our study. It is possible that the nude mice with orthotopic NPC growth and metastasis did not live long enough for liver metastasis to develop because this may be a later event.

Bright GFP fluorescence enabled imaging of NPC growth and metastases in orthotopic models. Host vessels induced in the growing tumor could be distinguished clearly against the background of the brilliant fluorescent tumor. Vessel development could be closely followed and quantified in real time, demonstrating the relationship of angiogenesis and cancer progression.

The imageable orthotopic model of NPC should play a critical role in elucidating the mechanisms involved in the growth, progression, metastasis, and angiogenesis of NPC and for evaluation of novel compounds with potential efficacy.

References

1. Chang ET, Adami H-O. The enigmatic epidemiology of nasopharyngeal carcinoma. Cancer Epidemiol Biomarkers Prev 2006;15:1765–77.
2. Cao SL. Biological characteristics of tumor growth delay in human nasopharyngeal carcinoma xenograft (NPC-837) after irradiation. Zhonghua Zhong Liu Za Zhi 1992;14:327–30.
3. Tang YY, Zhao SP, Xu J, Zhong Y, Xiao JY. Combining FCU/5-FU suicide gene/prodrug system and radiation in treating nasopharyngeal carcinoma: an experimental study. Zhonghua Bing Li Xue Za Zhi 2006;35:483–7.
4. Mai HQ, Zeng ZY, Feng KT, et al. Therapeutic targeting of the endothelin a receptor in human nasopharyngeal carcinoma. Cancer Sci 2006;97:1388–95.
5. Li GP, Huang K, Zhang H. Efficacy of 188Re-herceptin radioimmunotherapy in nude mouse model of nasopharyngeal carcinoma. Nan Fang Yi Ke Da Xue Xue Bao 2006;26:459–62.
6. Hoffman RM. Orthotopic metastatic mouse models for anticancer drug discovery and evaluation: a bridge to the clinic. Invest New Drugs 1999;17:343–59.
7. Bouvet M, Yang M, Nardin S, et al. Chronologically-specific metastatic targeting of human pancreatic tumors in orthotopic models. Clin Exp Metastasis 2000;18:213–8.
8. Budinger TF, Benaron DA, Koretsky AP. Imaging transgenic animals. Annu Rev Biomed Eng 1999;1:611–48.
9. Flotte TR, Beck SE, Chesnut K, Potter M, Poirier A, Zolotukhin S. A fluorescence video-endoscopy technique for detection of gene transfer and expression. Gene Ther 1998;5:166–73.
10. Fu XY, Besterman JM, Monosov A, Hoffman RM. Models of human metastatic colon cancer in nude mice orthotopically constructed by using histologically intact patient specimens. Proc Natl Acad Sci U S A 1991;88:9345–9.
11. Sun FX, Sasson AR, Jiang P, et al. An ultra-metastatic model of human colon cancer in nude mice. Clin Exp Metastasis 1999;17:41–8.
12. Hoffman RM. The multiple uses of fluorescent proteins to visualize cancer *in vivo*. Nat Rev Cancer 2005;5:796–806.
13. Hoffman RM, Yang M. Subcellular imaging in the live mouse. Nature Protocols 2006;1:775–82.
14. Hoffman RM, Yang M. Color-coded fluorescence imaging of tumor-host interactions. Nature Protocols 2006;1:928–35.
15. Hoffman RM, Yang M. Whole-body imaging with fluorescent proteins. Nature Protocols 2006;1:1429–38.
16. Ferrara N, Kerbel RS. Angiogenesis as a therapeutic target. Nature 2005;438:967–74.
17. Kerbel RS. A cancer therapy resistant to resistance. Nature 1997;390:335–6.
18. Chen HX, Mooney M, Boron M, et al. Phase II multicenter trial of bevacizumab plus fluorouracil and leucovorin in patients with advanced refractory colorectal cancer: an NCI Treatment Referral Center Trial TRC-0301. J Clin Oncol 2006;24:3354–60.
19. Paget S. The distribution of secondary growths in cancer of the breast. Lancet 1889;1:99–101.